Delayed Fluorescence Due to Annihilation of Triplets Produced in Recombination of Photo-Generated Ions

G. Angulo,*,†,‡ G. Grampp,† A. A. Neufeld,§,|| and A. I. Burshtein*,§

Institute of Physical and Theoretical Chemistry, Graz University of Technology, Graz, Austria, and Department of Chemical Physics, Weizmann Institute of Science, 76100 Rehovot, Israel

Received: January 30, 2003; In Final Form: June 20, 2003

In a previous article (*J. Chem. Phys.* **2002**, *116*, 2472), the nontrivial viscosity dependence of the geminate recombination efficiency was theoretically studied and briefly shown experimentally. Now, the experiments performed are reported in detail. Furthermore, the multistage kinetics of the fluorescence quenching by electron transfer to impurities is subjected to exhaustive experimental study and well fitted theoretically using integral encounter theory (IET) of the bimolecular reactions in solution. The quantum yields of free ions and triplet excitations are calculated and their nontrivial viscosity dependence is specified as well as the asymptotics of the bimolecular recombination of both ions and triplets. The annihilation of triplets results in a restoration of singlet excitations responsible for the delayed fluorescence.

I. Introduction

The irreversible electron transfer to the instantaneously excited singlet state of the acceptor molecule, ^{1}A*, from one of the electron donors D initiates the geminate recombination of the generated ion pair [D$^{\bullet+}$...A$^{\bullet-}$] to either the ground or excited triplet state of neutral products, [D...A] or [D... ^{3}A*]. This alternative makes the reaction scheme more complex than that studied earlier[1] because not only free ions are produced by light excitation, but also the triplet products of charge recombination, ^{3}A*:

$$\begin{array}{ccccc} & [D...{}^3A^*] & & D + {}^3A^* & \\ & \Uparrow \bar{\varphi}_T & & \Uparrow k_{RT} & \\ D + {}^1A^* \overset{W_i}{\Rightarrow} & [D^{\bullet+}...A^{\bullet-}] & \overset{\bar{\varphi}}{\rightarrow} & D^{\bullet+} + A^{\bullet-} & \quad (1.1) \\ I_0 \uparrow\downarrow \tau_r^0 & \Downarrow \bar{\varphi}_G & & \Downarrow k_{RS} & \\ A & [D...A] & & D + A & \end{array}$$

Biexcitonic annihilation of these triplets restores the singlet donor excitation which manifests itself by delayed fluorescence and starts again ionization (1.1) in the encounters with neutral acceptors. The chemiluminescence[2] and the electrogenerated chemiluminescence[3] due to triplet−triplet annihilation was many times studied. This stage represented by a scheme

$$3A^* + 3A^* \begin{cases} \xrightarrow{k_{TT}} {}^1A^* + {}^1A \\ \xrightarrow{3k_{TT}} {}^3A^* + {}^1A \end{cases} \quad (1.2)$$

was also incorporated in a total process of energy dissipation after primary singlet excitation followed by photoinduced electron transfer. This was done for either intermolecular[4] or intramolecular[5] electron transfer, but in neither case, the total kinetics of such a multi-stage reaction acquired the quantitative description which becomes possible only now, on the basis of IET equations.[6]

After the geminate stage of the reaction is accomplished we have two sorts of reactive particles in solution: ions with concentration $N^- = [D^{\bullet+}] = [A^{\bullet-}]$ and triplets with $T = [^3A^*]$. They are products of the dissociation and recombination of the ion pairs produced with a quantum yield ψ by forward electron transfer. The fraction of ions is $\psi\bar{\varphi}$, and that of triplets is $\psi\bar{\varphi}_T$, where $\bar{\varphi}$ is the charge separation quantum yield[7] and $\bar{\varphi}_T$ is the triplet quantum yield. The sum of the quantum yields of ions, triplets, and ground state neutral products is evidently equal to unity: $\bar{\varphi} + \bar{\varphi}_T + \bar{\varphi}_G = 1$. The subsequent bimolecular ion recombination and triplet annihilation start with the following initial concentration of the reactants at experimental $t = 0$ (after the geminate stage is over): $N^- = \psi\bar{\varphi}N^*(0)$ and $T(0) = \psi\bar{\varphi}_T N^*(0)$, where $N^*(0)$ is the initial value of singlet excited-state concentration $N^* = [^1A^*]$ produced by absorption of δ-pulse light.

In this work, we measured the kinetics of free ion recombination, $N^-(t)$, triplet annihilation, $T(t)$, and singlet excitation quenching, $N^*(t)$. From their initial values, we found $\bar{\varphi}$ and $\bar{\varphi}_T$ their viscosity dependence is one of the main goals of the present paper. Another important goal is the kinetics of the reactants recombination and delayed fluorescence resulting from triplet annihilation. We studied the fluorescence quenching by means of steady-state and time-resolved spectroscopy. From the former, the Stern−Volmer rate constant was obtained in the low concentration limit. When that concentration is increased, the Stern−Volmer plots start to deviate from linearity, more remarkably with increasing viscosity. This effect is attributed to the nonstationary diffusion effect. From the latter, we recovered the stationary rate constants (infinite time limit of the time-dependent rate constant) and analyzed the full decay curves with the Smoluchowski approach with an effective reaction radius.

The outline of this article is the following. In section III, we will estimate the rate of forward electron transfer, $W_i(r)$, using our experimental data and available energy information. In

* To whom correspondence should be addressed.
† Graz University of Technology.
‡ Part of the PhD thesis of G.A.
§ Weizmann Institute of Science.
|| On leave to the Max Planck Institut for Biophysical Chemistry, Göttingen, Germany.

10.1021/jp0342475 CCC: $25.00
Published on Web 08/19/2003

section IV, the efficiency of geminate ion recombination will be reported and its nonmonotonic viscosity dependence discussed qualitatively in our previous article[1] will be fitted quantitatively. In section V, the obtained viscosity dependence of the triplet quantum yield will also be explained using the contact approximation for backward electron transfer. In the same section, the complex kinetics of charge and triplet recombination will be considered jointly in the framework of the Markovian simplification of IET equations. The long time asymptotics of the process will be treated analytically, and from the best numerical fit to the experimental data, all of the rate constants will be specified.

II. Experimental Procedures

To change the viscosity of the samples without changing any other macroscopic physical property of the solvent, dimethyl sulfoxide (DMSO)−glycerol mixtures were used. These mixtures show a perfect miscibility in the whole molar fraction range used and almost a constant refraction index, as well as a similar high dielectric constant.[8] Electron-transfer quenching of perylene (PER) by N,N′-dimethylaniline (DMA) is a well studied photochemical system which is widely used.[9]

PER (Aldrich, 99.5+%) and glycerol (Aldrich 99.8%, <0.1% H_2O) were used as received. DMA (Aldrich, >99%) was distilled under reduced pressure (17 mbar, 77 °C) and always handled under argon. DMSO (Fluka, 0.05% H_2O) was twice crystallized by freezing cycles.[10] The concentrations of PER, 2×10^{-5} M, and of the DMA, 0.033 M, were kept constants throughout all of the laser flash photolysis experiments. For the calibration of the laser energy, triplet−triplet absorption decay curves of tetracene solutions in cyclohexane (dried dynamically with a 4 Å molecular sieve and distilled) were recorded simultaneously to the experiments, giving an optical density of around 0.35, like the sample, at 441 nm. Absorption, emission, and the lifetime equipment used has already been described.[11] The laser system used was a pulsed dye laser (Lambda Physics model FL 105; coumarine 120/ethanol; emission at 441 nm; energy conversion factor of 15%) pumped by an XeCl-excimer laser (Lambda Physics model Compex 120; 308 nm; 100 mJ; 10 ns pulse width). Typical energies in the sample were of 2−3 mJ. For the transient detection, the continuous light of a tungsten lamp (12 V; 100 W) was focused perpendicularly to the excitation. Detection was made by a OBB/PTI monochromator model 101/102 fixed at the proper wavelength. The signals were detected by a Hamamatsu R928P photomultiplier working at 5 kΩ with 800 V connected to a 9350C LeCroy digital storage oscilloscope. All of the samples were purged with Ar during at least 40 min in a reservoir connected to a 1 × 1 cm flow-through cell to avoid any problems due to the photodecomposition of the reactants. Typical flow rates were 5 mL/min. After the laser experiments, the kinematic viscosities were determined using a thermostated Ubbelohde viscosimeter, and the densities were measured with a commercial picnometer. The refraction index of the mixtures was measured with an Abbe refractometer at the sodium D line giving a constant value over the range employed of 1.478 ± 0.001. To check the microviscosity of the mixtures, we measured the fluorescence quantum yield of auramine O in the mixtures, matching our results quite well with the calibration curves for water−glycerol mixtures.[12] All of the measurements were done at 20.0 ± 0.1 °C.

The quenching experiments were performed as already reported,[11] but in a mixture of DMSO and glycerol, giving similar results.

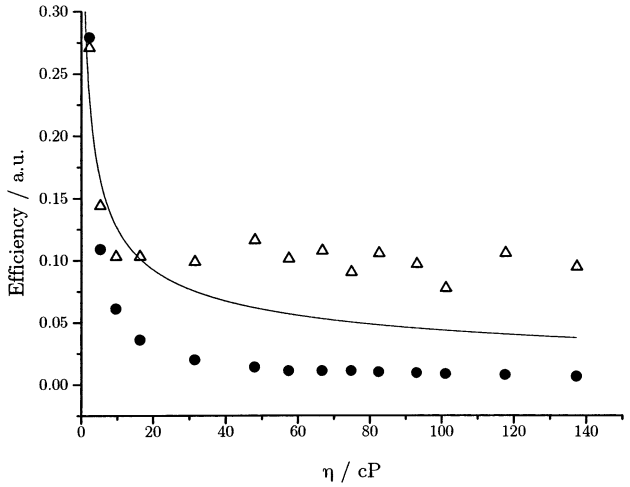

Figure 1. Laser flash photolysis results: efficiencies of PER anion production (circles) and of PER triplet production (triangles) against viscosity. The continuous line is the simulation performed with eq 5.2, with the values: $k_S = 2.6 \times 10^3$ Å^3 ns^{-1}; $k_{RS} = 2.07 \times 10^6$ Å^3 ns^{-1}; $k_{RT} = 1.97 \times 10^7$ Å^3 ns^{-1}.

The efficiency of the separation of the ions after the forward reaction is defined in the usual way:

$$\phi_{ion} = \bar{\varphi}_{rip}\bar{\varphi}; \text{ with } \bar{\varphi}_{rip} = \frac{k_q\tau_F^0[Q]}{1 + k_q\tau_F^0[Q]} \qquad (2.1)$$

where $\bar{\varphi}_{rip}$ and $\bar{\varphi}$ denote the formation of the radical ion pair and the separation of the ions quantum yields, respectively. ϕ_{ion} is the overall quantum yield of the formation of ions, k_q is the Stern−Volmer quenching rate constant and τ_F^0 the fluorescence lifetime of the PER without quencher. Experimentally, the quantum yields are determined by comparison of the transient absorptions of the PER radical anion with the triplet state of tetracene:

$$\phi_{ion} = \phi_{S-T}\frac{A_{580}^{Per-}/\epsilon_{580}^{Per-}}{A_{485}^{^3T}/\epsilon_{485}^{^3T}}\frac{1 - 10^{-A_{441}{}^{T}}}{1 - 10^{-}A_{441}{}^{Per}} \qquad (2.2)$$

The first term is the singlet−triplet intersystem crossing quantum yield of the tetracene (0.63),[13] the second is the ratio between the PER free radical anion ($\epsilon_{580}^{Per\bullet-} = 50\,000$ M^{-1}cm^{-1})[14] and the tetracene triplet concentrations ($\epsilon_{485}^{^3T} = 245\,000$ M^{-1} cm^{-1})[13] at experimental time zero after the laser excitation. The last one is a correction due to the different optical densities of the reference and the probe samples at 441 nm, the excitation wavelength.

The triplet−triplet absorption of PER was measured at 485 nm ($\epsilon_{485}^{^3Per} = 140\,000$ M^{-1}cm^{-1})[15] for the determination of its formation quantum yield, $\bar{\varphi}_T$ (Figure 1). The equivalent equations to (2.1) and (2.2) were used to calculate this quantity but from the triplet−triplet absorption. The transient absorption spectrum (Figure 2) was recorded from 455 to 640 nm showing two peaks. One is attributed to the triplet state, very similar in shape to the spectrum published by Löhmannsröben et al.[14] The absorption of the DMA cation can be neglected because its extinction coefficient is small (less than 4000 M^{-1}cm^{-1} in solid matrixes).[16]

III. Irreversible Fluorescence Quenching by Electron Transfer

A. The Diffusion Coefficient. On fitting the experimental data of the fluorescence quenching and the laser flash photolysis,

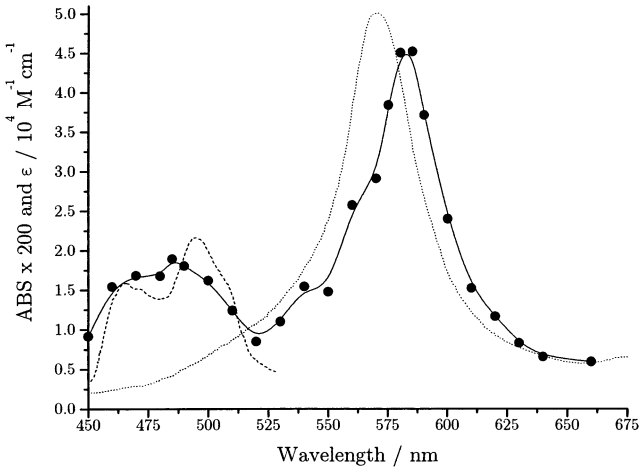

Figure 2. Transient absorption spectrum after laser excitation of a DMSO solution of PER and DMA (circles). The dashed and the dotted lines are the T−T absorption and the PER anion absorption spectra, respectively, reproduced from the literature. The vertical axis represents the "time zero" absorption recorded by us, times 200, and simultaneously, the extinction coefficients are borrowed from literature.

a fundamental parameter is the diffusion coefficient. It can be used either as a given input parameter or left free during the fitting procedures. In our opinion, the latter strategy is not desirable because of the complexity of the problem. Therefore, it is better to measure the diffusion coefficient or to make use of the best models available to calculate it. In the latter case, the choice of the model is critical, and the use of the Stokes−Einstein equation for D

$$D_x = \frac{k_B T}{f_x r_x 6\pi\eta} \tag{3.1}$$

in the usual manner (stick boundary conditions, $f_x = 1$) did not give good results in our case. Using slip boundary conditions ($f_x = 2/3$) improved slightly the results, but the best ones were obtained using the Spernol−Wirtz model for the friction coefficient:[17]

$$f_x = \left(0.16 + 0.4\frac{r_x}{r_s}\right)(0.9 + 0.4T_r^x - 0.25T_r^6), \quad T_r = \frac{T - T_f}{T_b - T_f} \tag{3.2}$$

where x denotes the solute and s the solvent and T_r is a reduced temperature, with T_b and T_f as the boiling and freezing temperatures and T as the working temperature. The reduced temperature of the solvent mixtures was calculated as the weighted average of the components reduced temperatures. An average radius of 2.5 Å is used for the solvent. The radii of the reactants were calculated from AM1 semiempirical geometry optimization with an ellipsoid model and elliptic integrals of the first kind.[18] The same diffusion coefficient was used for the neutral reactants and the charged products.

B. Time-Resolved Quenching. The fluorescence intensity is proportional to the density of excited states N^* which decays nonexponentially after d-pulse excitation. In differential encounter theory (DET) the kinetics of the excitation kinetics is given by[7]

$$N^*(t) = N^*(0)\exp\left(-\frac{t}{\tau_F^0} - [Q]\int_0^t k_1(t')\,dt'\right) \tag{3.3}$$

where $k_I(t)$ is the time dependent rate constant of the forward

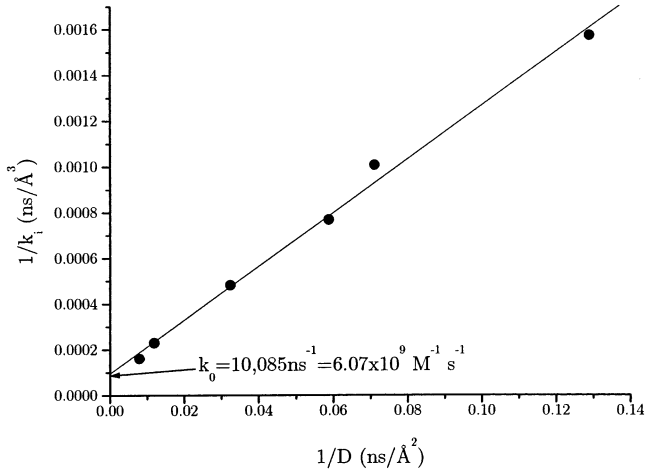

Figure 3. Inverse ionization rate constant calculated from eq 3.5 with the experimental R_{eff} presented in Figure 4, against the inverse diffusion coefficient. From the extrapolation to zero in the low viscosity region, $k_0 = 6.07 \times 10^9$ M^{-1} s^{-1} is extracted.

electron transfer (ionization). Its long time nonstationary behavior obeys the Smoluchowsky law with effective reaction radius R_{eff} substituted for the contact one. Being integrated in eq 3.3, it leads to the following long time asymptote of excitation decay:[19]

$$N^*(t) = N^*(0)\exp\left(-t\left(\frac{t}{\tau_F^0} + 4\pi R_{eff} D[Q]\right) - t^{1/2}8(\pi D)^{1/2}(R_{eff})^2[Q]\right) \tag{3.4}$$

Fitting this expression for our single photon counting curves for different quencher concentrations and viscosities, we get R_{eff} for all of them and calculated the asymptotic (Markovian) rate constant

$$k_i = \lim_{t\to\infty} k_I(t) = 4\pi R_{eff} D \tag{3.5}$$

The viscosity (diffusional) dependence of this quantity can be now fitted with conventional theoretical models of electron-transfer rate $W_I(r)$ used to calculate k_i.

The oldest and most popular is the Collins−Kimball model of contact reaction.[20] In its generalized version proposed in ref 21

$$W_I(r) = \frac{k_0}{4\pi\sigma^2}\delta(r - R) \tag{3.6}$$

where R is the fitting parameter and k_0 is the kinetic rate constant. The Collins−Kimball model is valid at low viscosities

$$1/k_i = 1/k_0 + 1/4\pi RD \tag{3.7}$$

Fitting this linear dependence to our data (Figure 3), we were able to find k_0 from the interception of its extrapolation with ordinate. It appeared to be

$$k_0 = 10085\ \text{Å}^3\ \text{ns}^{-1} = 6.07 \times 10^9\ \text{M}^{-1}\ \text{s}^{-1} \tag{3.8}$$

Another popular model assumes that the transfer is remote and its rate vanishes exponentially with inter-reactant distance:[7]

$$W_I(r) = W_c e^{-2(r-\sigma)/l} \tag{3.9}$$

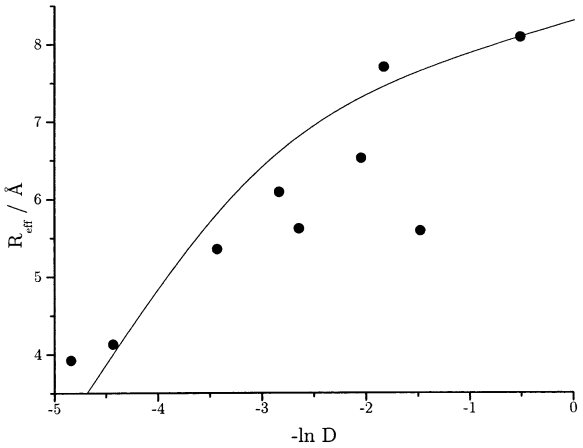

Figure 4. Effective quenching radius as a function of the natural logarithm of the diffusion coefficient (in Å²/ns). Circles, experimental points; solid line, fit performed with eq 3.10. The contact radius was fixed to 7.2 Å. The contact rate obtained is $W_c = 29.12$ ns^{-1} and the tunneling distance $l = 0.81$ Å.

This model takes into account that R_{eff} exceeds R at high viscosity and increases with a further decrease of D according to the following law:[7,22]

$$R_{\text{eff}} = \sigma + \frac{l}{2}\left[\ln(\gamma^2\beta_{\text{m}}) + 2\varphi\left(\beta_{\text{m}}\frac{2\sigma}{l}\right)\right] \qquad (3.10)$$

with

$$\theta(x,y) = \frac{K_0(2\sqrt{x}) - y\sqrt{x}K_1(2\sqrt{x})}{I_0(2\sqrt{x}) + y\sqrt{x}I_1(2\sqrt{x})},$$

$$\beta_{\text{m}} = \frac{W_c l^2}{4D}\,\gamma = \mathrm{e}^C \approx 1.781$$

where C is the Euler constant and $K(x)$ and $I(x)$ are the modified Bessel functions. The fitting parameters of eq 3.10, l and b_{m}, originate from two parameters of the rate (3.9), l and W_{c}. This makes the determination of them by the least-squares fitting rather uncertain.[23] Because of the same reason in ref 24, one parameter was set equal to the "value usually admitted in the literature", and only another was obtained from the best fit. We are in a better position. Having in hand

$$k_0 = \int_\sigma^\infty 4\pi r^2 W_{\text{i}}(r)\,\mathrm{d}r = 2\pi W_{\text{c}}(\sigma^2 l + \sigma l^2 + l^3/2) \qquad (3.11)$$

we relate W_{c} to l and can vary only the latter. The result of our fitting shown in Figure 4 is the following:

$$l = 0.81 \text{ Å}, \quad W_{\text{c}} = 29.12 \text{ ns}^{-1}$$

Even the exponential model of $W_{\text{I}}(r)$ is not the best. More reliable is the Marcus expression for the nonadiabatic electron-transfer rate:[7]

$$W_{\text{I}}(r) = {V_0}^2 \exp\left(-\frac{2(r-\sigma)}{L}\right)\sqrt{\frac{\pi}{\lambda T}}\exp\left(-\frac{(\Delta G_{\text{I}} + \lambda)^2}{4T\lambda}\right) \qquad (3.12)$$

where ΔG_{I} and l are the free energy and reorganization energy of transfer, L is the true distance of tunneling, and V_0 is the matrix element of it at contact. In the near vicinity of contact this Marcus formula can be approximated by the exponential model if one sets

$$W_{\text{I}}^{\text{Marcus}}(\sigma) = W_{\text{I}}^{\text{Exp}}(\sigma) \text{ and } \left.\frac{\mathrm{d}W_{\text{I}}^{\text{Marcus}}}{\mathrm{d}r}\right|_{r=\sigma} = \left.\frac{\mathrm{d}W_{\text{I}}^{\text{Exp}}}{\mathrm{d}r}\right|_{r=\sigma}$$

Making such an identification, we obtained for the true tunneling distance $L = 1.38$ Å which is less than 1.6 Å found in ref 21 and even smaller than 2 Å arbitrarily chosen in ref 24 as a conventional one. We guess that the smaller values of L are more reliable because they are closer to the quantum-mechanical estimate of this decrement in free space.[25]

C. Stern−Volmer Constant. Under permanent illumination, the relative quantum yield Ψ was measured (the ratio of the yields with and without quenchers). This quantity obeys the Stern−Volmer law:[7,26]

$$\frac{1}{\Psi} = \frac{N^*(0)\tau_{\text{F}}^0}{\int_0^\infty N^*(t)\,\mathrm{d}t} = 1 + k_{\text{q}}\tau_{\text{F}}^0[Q] \qquad (3.13)$$

where the Stern−Volmer constant k_{q} is actually a function of $[Q]$ at high concentrations.[27] However, below 0.1 M, we observed no deviations from the linear concentration dependence of $1/\Psi$. The region of linearity is reduced with increasing viscosity down to 0.05 M at 140 cP. The experimental values of k_{q} as a function of viscosity are plotted in Figure 5 as full circles. The same dependence of the stationary rate constant, $k_i(h)$, represented by triangles, is quite different.

This was expected because there should be a significant contribution of nonstationary quenching in the Stern−Volmer constant especially at high viscosities. To support this statement, we calculated Ψ from eq 3.13 using there N^* from eq 3.3 with the contact estimate of $\int_0^{\text{t}} k_{\text{I}}(t')\,\mathrm{d}t'$. The latter is provided by the integrated Collins−Kimball equation[23]

$$\int_0^t k_{\text{I}}(t')\,\mathrm{d}t' = \frac{k_{\text{D}}k_0}{k_{\text{D}} + k_0}\left\{\text{t} + \frac{k_0}{k_{\text{D}}a^2}[\exp(a^2 t)\,erfc(at^{1/2}) + 2a(t/\pi)^{1/2} - 1]\right\}$$

$$a = {\tau_{\text{D}}}^{-1/2}\left(1 + \frac{k_0}{k_{\text{D}}}\right),\ \tau_{\text{D}} = \sigma^2/D \qquad (3.14)$$

with the kinetic rate constant (3.8). The results (open circles) are quite consistent with those obtained experimentally.

IV. Efficiency of Geminate Ion Recombination

As it has been already shown in our former article,[1] the viscosity dependence of the geminate recombination efficiency Z can be easily calculated by means of integral encounter theory (IET). The integro-differential equations of IET determine the time evolution of the excitation and ion populations after δ-pulse:[1,28]

$$\dot{N}^*(t) = [Q]\int_0^t R^*(\tau)N^*(t-\tau)\,\mathrm{d}\tau - N^*(t)/\tau_{\text{F}}^0 \qquad (4.1a)$$

$$\dot{N}^-(t) = [Q]\int_0^t R^{\dagger}(\tau)N^*(t-\tau)\,\mathrm{d}\tau \qquad (4.1b)$$

where the kernels (memory functions) substitute for the ordinary

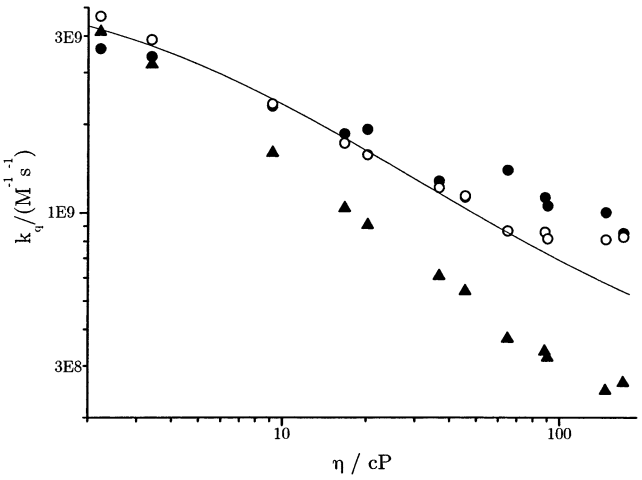

Figure 5. Viscosity dependence of the Stern−Volmer rate constant (solid circles), of the stationary rate constant (solid triangles). The open circles represent the integral-CK result, borrowing the static rate constant from our experimental results and the continuous line represents the IET kernel obtained simultaneously and with the same parameters as the line in Figure 4.

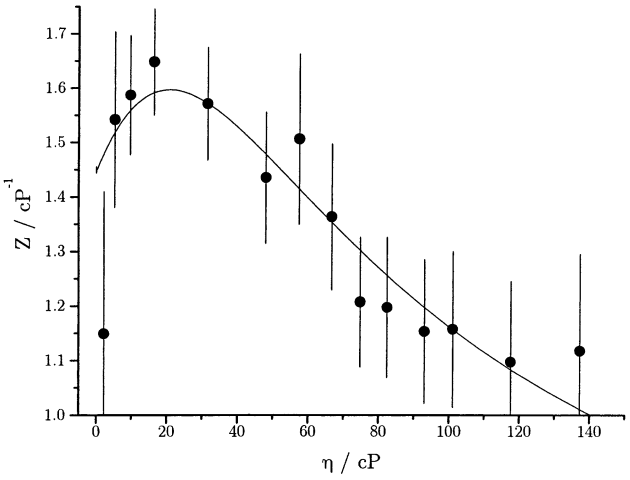

Figure 6. Recombination efficiency as a function of viscosity. The continuous line represents the best obtained simulation with IET equations, with the following parameters: contact radius = 7.2 Å; tunneling length = 1.38 Å; ionization preexponential factor = 1.2×10^{11} ns^{-1}; contact ionization energy = −0.56 eV; contact recombination energy = −2.27 eV; outer-sphere reorganization energy = 0.85 eV; ionization inner-sphere reorganization energy = 0.13 eV; recombination inner-sphere reorganization energy (low frequency) = 0.24 eV recombination preexponential factor = 4.75×10^{12} ns^{-1}; vibronic quant = 7.2×10^{-3} eV; quantum mode reorganization energy = 1.04 eV; number of quantum modes = 30.

rate constants. Their Laplace transformations are defined as follows:

$$\tilde{R}^*(s) = (s + 1/\tau_F^0) \int W_I(r)\tilde{\nu}(r;s)\, d^3r \qquad (4.2a)$$

$$\tilde{R}^\dagger(s) = (s + 1/\tau_F^0) \int [W_I(r)\tilde{\nu}(r;s) - W_R(r)\tilde{\mu}(r;s)]\, d^3r \qquad (4.2a)$$

The pair correlation functions obey the following auxiliary equations:[7,28]

$$[s + 1/\tau_F^0 + W_I + \hat{L}_r]\tilde{\nu}(r;s) = 1$$

$$[s + W_R + \hat{L}_r']\tilde{\nu}(r;s) = W_I\tilde{\nu}(r;s)$$

where $\hat{L}_r$ and $\hat{L}_r'$ are the diffusional operators. Because in our case the ionization takes place in the normal Marcus region and the recombination in the inverted one, the ionization rate can be represented by a single channel formula (3.12), but for the recombination rate, we need its multichannel analog:[7]

$$W_R(r) = V_0^2 \exp\left(-\frac{2(r-\sigma)}{L}\right)\sqrt{\frac{\pi}{\lambda T}}\sum_{-\infty}^{\infty}\frac{e^{-S}S^n}{n!} \times \exp\left(-\frac{(\Delta G_R(r) + \lambda(r) + \hbar\omega n)^2}{4T\lambda(r)}\right) \qquad (4.3)$$

where the Huang−Rhys factor[29] $S = \lambda_q/\hbar\omega$ is a ratio of the quantum mode reorganization energy λ_q and its frequency ω. The space dependence of the solvent reorganization energy λ, as well as of the free energy of transfer was already specified elsewhere.[1,7] We must just point out that the inner-sphere reorganization energy has been estimated by Nelsen's method with semiempirical AM1 calculations,[30] and it is different for the forward (0.13 eV) and for the recombination (0.24 eV) processes.

As the backward electron transfer to ground state takes place in the Marcus inverted region, the reaction layer is shifted away from contact. Therefore, the recombination depends dramatically on where the ions were born by the preceding ionization: inside or outside this layer. However, their initial distribution depends in turn on encounter diffusion of neutral reactants participating in the bimolecular forward electron transfer. Hence, the diffusion and elementary events are not separable. The experimental quantities, $\bar{\varphi}$, the charge separation quantum yield, and κ, the "ideal" (low concentration) Stern−Volmer constant are related to the kernels in the following way:

$$\bar{\varphi} = \tilde{R}^\dagger(0)/\tilde{R}^*(0) \qquad (4.4a)$$

$$k_q = \tilde{R}^*(0) \qquad (4.4b)$$

Hence, only the Laplace transformed kernels with argument zero have to be calculated, reducing the complexity of the simulation.

Instead of studying directly the charge separation yield, it is more straightforward and instructive to discuss the viscosity behavior of the recombination efficiency

$$Z(D) = D\left[\frac{1}{\bar{\varphi}} - 1\right] \qquad (4.5)$$

In the primitive exponential model, this quantity does not depend on diffusion and relates only to the recombination rate k_{rec} which is homogeneous within the transparent reaction sphere: $Z = k_{rec}/4\pi\sigma$ = const.[7] In reality, this is rarely the case. The measured Z shown in Figure 6 indicates that there is a pronounce viscosity dependence of this quantity that was explained qualitatively in a few former articles.[1,7,28] The simulation of these data with the IET expression (4.4a) used in (4.5) fits them rather well. Not less successful is the fitting also of k_q with the IET expression (4.4b) shown by the solid line in Figure 5. A reasonable agreement between IET and the experimental data was obtained with the sensible parameters listed in the figure captions. The tunneling distance was obtained from the analysis of the viscosity dependence of the effective radius of quenching. The preexponential factor in eq 3.12, $V_0^2 = \sqrt{\pi/\lambda(\sigma)T}$, was extracted by using the experimental value of k_0, eq 3.8, in its general definition (3.11). The solvent reorganization energy is slightly smaller than that usually obtained with the simple Born approximation. The contact radius is almost the same as the calculated one, and the tunneling distance is quite reasonable.

V. Creation and Annihilation of Triplets

A. Triplet Absorption Spectrum. Leonhardt and Weller recognized almost 40 years ago that as a product of the electron-transfer reaction between PER and DMA the triplet state of the fluorophor appears.[31] In our laser-flash photolysis experiments, we also observe the absorption due to this state. In Figure 2, the transient absorption spectrum at experimental "time zero" is compared to the spectrum published by the authors referred to above. The shape of our spectra coincides well with that obtained by Löhmannsröben et al.,[14] because of the use of a similar wavelength discrete recording method. Although the contribution to the signal at the T−T absorption maximum (485 nm) of the DMA radical cation[16] is almost negligible, it was also considered for the sake of correction.

B. Triplet Geminate Production Efficiency. A complete and coherent description of the geminate production of the PER in the triplet state from the recombination of ions is nowadays not possible in the frame of noncontact kinetic equations. To do it rigorously, the full set of Liouville equations describing the whole spin system should be derived, accounting for the distance dependence of the mixing Hamiltonian coupled to the diffusion equations. This task has been recently solved in the contact approximation[32a] and applied to this problem.[32b] The spin mixing was considered to take place stochastically, characterized by a rate constant k_S: The rest of the constants

$$\begin{array}{ccc} {}^1[D^{\bullet+}\ldots A^{\bullet-}] & \underset{k_S}{\overset{3k_S}{}} & {}^3[D^{\bullet+}\ldots A^{\bullet-}] \\ \downarrow k_{RS} & & \downarrow k_{RT} \\ {}^1D + {}^1A & & {}^1D + {}^3A^* \end{array} \qquad (5.1)$$

are given by their kinetic values, k_{RS}, for recombination to the ground singlet state and k_{RT} for the recombination to the triplet state. The quantum yield of contact triplet production was found to be

$$\bar{\varphi}_T = \frac{k_D k_{RT}\sqrt{k_S\tau_D}}{k_D(k_{RT}-k_{RS})\sqrt{k_S\tau_D} + {}^2/_3(k_D+k_{RS})[k_{RT}+k_D(1+2\sqrt{k_S\tau_D})]} \qquad (5.2)$$

Obviously, this contact approximation is too rough to explain the experimental data at high viscosities in all the details, because the ions initial distribution function moves away from contact the higher the viscosity (see solid line in Figure 1).

C. Delayed Fluorescence and Long Time Kinetics. As a result of the production of triplets, we could observe delayed fluorescence due to the triplet−triplet annihilation process, as already represented in eq 1.2. From the energetical point of view, the repopulation from the triplets of the excited single state is feasible, being the lowest triplet energy of PER 1.55 eV.[33] Taking into account the Wigner−Witmer spin conservation rules, five different species could be formed after the T−T annihilation:[34] ^{5}A*, normally energetically not accessible, ^{3}A**, that decays very fast to the lowest triplet state ^{3}A*, ^{1}A*, that gives rise to the delayed fluorescence, and the ground state ^{1}A. To detect the delayed fluorescence signal a high excitation intensity must be used to create a high enough triplet concentration. In pure DMSO, their initial concentration is of about 10^{-8} M. This is enough to create excited singlets sufficient for delayed fluorescence. In Figure 7A, the dissipation of triplets and anions are shown, whereas in Figure 7B, the long-time kinetic traces

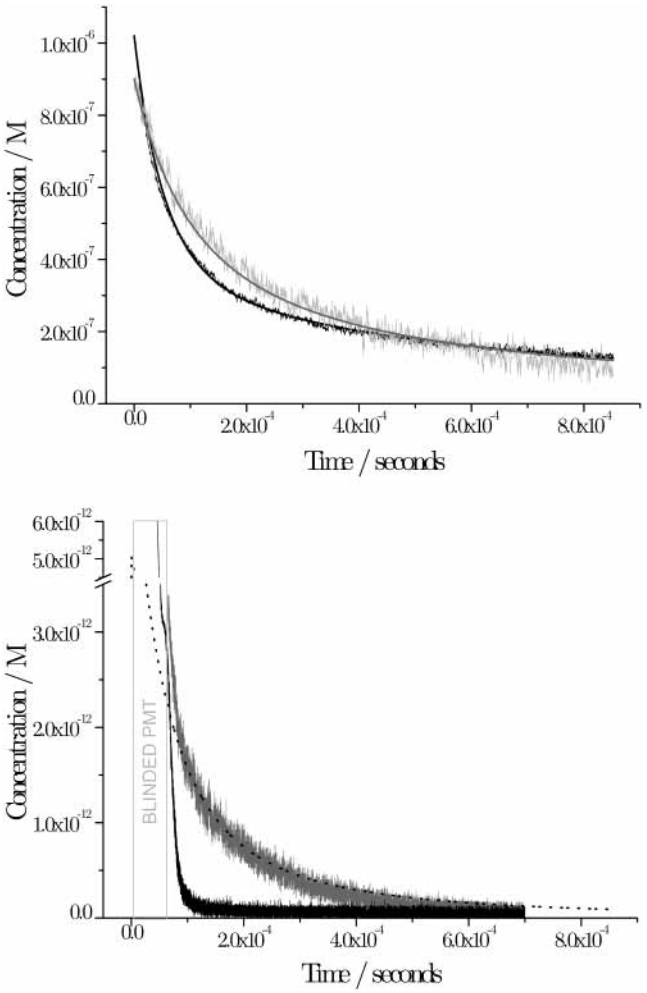

Figure 7. Long time kinetics of the PER anion (black), triplet (grey) (A) and the observed delayed fluorescence (grey), together with the signal received without quencher (black) (B). The dotted lines represent the best fit obtained with the eq 5.3. The values for the rates are $k_S = 1.818 \times 10^9 s^{-1}$; $k_Q = 3.6 \times 10^9$ M^{-1} s^{-1}; $k_{TT} = 2.24 \times 10^9$ M^{-1} s^{-1}; $k_{BT} = 2.35 \times 10^9$ M^{-1} s^{-1}; $k_{BS} = 4.85 \times 10^9$ M^{-1} s^{-1}; $k^{e-} = 6 \times 10^3$ s^{-1}; $k_B^{e-} = 3.50 \times 10^9$ M^{-1} s^{-1}.

of the delayed fluorescence, recorded at 475 nm, are also shown. To compare the delayed fluorescence signal with the response of the apparatus, the signal due to a sample of the same PER concentration without DMA is shown. At times longer than 60 μs, the photomultiplier is completely recovered from saturation caused by the intense fluorescence, even in the absence of quencher; therefore, any apparative artifact can be readily ruled out.

The following Markovian kinetic equations were used for fitting the experimental results shown in Figure 7:

$$\frac{\partial[^1A^*]}{\partial t} = -1/\tau_F^0[^1A^*] - k_i[^1A^*][^1D] + k_{TT}[^3A]^2 \qquad (5.3a)$$

$$\frac{\partial[^3A]}{\partial t} = k_F^0[^2A^{\bullet-}] - [^2A^{\bullet+}] - 5k_{TT}[^3A]^2 - k_T[^3A] \qquad (5.3b)$$

$$\frac{\partial[^2A^{\bullet-}]}{\partial t} = \bar{\varphi}k_i[^1A^*][^1D] - (k_B^T + k_B^S)[^2A^{\bullet-}][2D^{\bullet+}] - k^{e-}[^2A^{\bullet-}] + k_B^{e-}[e^-]\cdot[^1A] \qquad (5.3c)$$

where k_{TT} is the T−T annihilation rate constant, k_{BT} and k_{BS} are the recombination to the triplet and to the singlet states from

the free ions, k^{e-} is the electron ejection of the PER anion, caught by the solvent, and k_B^{e-} is the recombination of this "solvated electron" with the neutral PER. Without considering this additional channel of electron ejection, several times reported in the literature,[35] it is not possible to explain the kinetics of the anion, coupled to the triplets and of the delayed fluorescence. The ordinate in the delayed fluorescence plot is of course arbitrary and determined by the result of the fit, but what we were looking for was a complete description of the shape of this trace. Note that in the kinetic equations no consideration was taken for the very long distance character of the T−T annihilation that occurs via the Förster energy transfer. The rates obtained for this fit are listed in the figure caption.

VI. Conclusions

The viscosity dependence of the efficiency of ion separation after fluorescence quenching by electron transfer has been shown to be better understandable when appropriate coordinates are chosen: the efficiency of recombination, *Z*, against the mutual diffusion coefficient. In this way, the deviations from the exponential model predictions become evident. Only the encounter theory, used here in its integral version, can quantitatively explain its nonmonotonic behavior.

The time-resolved fluorescence decay curves, show deviations from exponentiality at short times which become more important for higher viscosity. It was possible to explain this with the long time approximation of the Smoluchowski theory. The positive deviations in the steady-state Stern−Volmer plots that rise up with viscosity have also been explained with the DET, demonstrating the occurrence of a nonstationary stage of the diffusion-assisted quenching reaction.

An additional recombination channel has to be considered: the recombination to the triplet state of the fluorophor. A contact result of the encounter theory for the geminate recombination to both states, ground and triplet, with stochastic spin mixing has been used to explain the qualitative viscosity change of the triplet efficiency.

The long time kinetics of the radical anion, the triplet state, and the excited-state population decays has been fitted in the frame of the Markovian kinetic equations. The delayed fluorescence has been recorded definitely and assigned as the result of the triplet−triplet annihilation process.

Acknowledgment. G.G. and G.A. acknowledge the financial support given by the Graz University of Technology, the Austrian Ministry of Education, Science and Culture and the Volkswagen Foundation (Germany) for this research project. G.A. thanks Daniel Kattnig for his help on programming the fits to the various problems treated in this article. The authors are grateful to Vladimir Gladkik for his computational assistance.

References and Notes

(1) Neufeld, A. A.; Burshtein, A. I.; Angulo, G.; Grampp, G. *J. Chem. Phys.* **2002**, *116*, 2472.

(2) Weller, A.; Zachariasse, K. In *Chemiluminescence and Bioluminescence*; Cormier, M. J., Hercules, D. M., Lee, J., Eds.; Plenum: New York, 1973. Zachariasse, K. Exciplezes in chemiluminescent radical ion recombination. In *The Exciplex*; Gordon, M., Ware, W. R., Eds.; Academic Press Inc.: New York, 1975. Weller, A.; Zachariasse, K. *Chem. Phys. Lett.* **1971**, *10*, 153.

(3) Feldberg, S. W. *J. Phys. Chem.* **1966**, *70*, 3298. Faulkner, L. R.; Tachikawa, H.; Bard, A. J. *J. Am. Chem. Soc.* **1972**, *94*, 691. Kapturkiewicz, A. J. *Electroanal. Chem.* **1994**, *372*, 101. Kapturkiewicz, A. In *Advances in Electrochemical Sciences and Engineering*; Alkire, R., Gerischer, H., Kolb, D. M., Tobias, C. W., Eds.; Wiley-VCH: Weinheim, Germany, 1997; Vol. 5, p 1. Ritchie, E. L.; Pastore P., Wightman, R. M. *J. Am. Chem. Soc.* **1997**, *119*, 11920.

(4) Lavrik, N. L.; Nechaev, O. V. *Chem. Phys.* **1988**, *124*, 273.

(5) Werner, U.; Kühnle, W.; Staerk, H. *J. Phys. Chem.* **1993**, *97*, 9280.

(6) Burshtein, A. I. *J. Lumin.* **2001**, *93*, 229.

(7) Burshtein, A. I. *Adv. Chem. Phys.* **2000**, *114*, 419.

(8) Bhattacharyya, B.; Wolff, J. *J. Biol. Chem.* **1984**, *259*, 11836.

(9) See, for example: Rehm, D.; Weller, A. *Isr. J. Chem.* **1970**, *8*, 259. Mataga, N.; Asahi, T.; Kanda, Y.; Okada, T. *Chem. Phys.* **1988**, *127*, 249. Lewitzka, F.; Löhmannsröben, H.-G. *Z. Phys. Chem. (N. F.)* **1990**, *169*, 181. Vauthey, E. *J. Phys. Chem. A* **2001**, *105*, 340.

(10) Kavakatsanis, C. G.; Reddy, T. B. In *IUPAC, Anal. Chem. Div. "Recommended Methods for Purification of Solvents and Tests for Impurities"*; Coetzee, J. F., Ed.; Pergamon Press: Oxford, 1982; p 25.

(11) Angulo, G.; Grampp, G.; Landgraf, S. *J. Inf Rec.* **2000**, *25*, 381. Landgraf, S. *Spectrochim. Acta* **2001**, *57A*, 2029.

(12) Hasegawa, M.; Sugimura, T.; Shindo, Y.; Kitahara, A. *Colloids Surf. A* **1996**, *109*, 305. (The last two curves of Figure 2 in this article were used. The first one was not correctly printed: Hasegawa's personal communication.)

(13) Jardon, P.; Gautron, R. *J. Chim. Phys.* **1988**, *82*, 353.

(14) Lewitzka, F.; Löhmannsröben, H.-G. *Z. Phys. Chem. (N. F.)* **1990**, *169*, 203.

(15) Bensasson, R.; Land, E. J. *Trans. Faraday Soc.* **1970**, *67*, 1904.

(16) Shida, T.; Nosaka, Y.; Kato, T. *J. Phys. Chem.* **1978**, *82*, 695.

(17) Spernol, A.; Wirtz, K. Z. *Naturforsch.* **1953**, *8a*, 522.

(18) Grampp, G.; Jaenicke, W. *Ber. Bunsen-Ges. Phys. Chem.* **1991**, *95*, 904.

(19) Rice, S. A. In *Comprehensive Chemical Kinetics "Diffusion-Limited Reactions"*; Bamford, C. H., Tipper, C. F. H., Compton, R. G., Eds.; Elsevier Science Publishers B. V.: Amsterdam, 1985; p 31.

(20) Collins, F. C.; Kimball, G. E. *J. Colloid Sci.* **1949**, *4*, 425.

(21) Gladkikh, V. S.; Burshtein, A. I.; Tavernier, H. L.; Fayer, M. D. *J. Phys. Chem. A* **2002**, *106*, 6982.

(22) Doktorov, A. B.; Burshtein, A. I. *Sov. Phys. JETP* **1975**, *41*, 671.

(23) Murata, S.; Nishimura, M.; Matsuzaki, S. Y.; Tachiya, M. *Chem. Phys. Lett.* **1994**, *219*, 200.

(24) Allonas, X.; Jacques, P.; Accary, A.; Kessler, M.; Heisel, F. *J. Fluoresc.* **2000**, *10*, 237.

(25) Kuznetsov, A. M.; Ulstrup, J. In *Tunneling*; Jortner, J., Pullman, B., Eds.; D. Reidel Publishing Company: Dordrecht, The Netherlands, 1986; pp 345−360.

(26) Stern, O.; Volmer, M. *Physik. Zeitschr.* **1919**, *20*, 183.

(27) Popov, A. V.; Gladkikh, V. S.; Burshtein, A. I (to be published).

(28) Burshtein, A. I.; Neufeld A. A. *J. Phys. Chem. B* **2001**, *105*, 12364.

(29) Huang, K.; Rhys, A. *Proc. R. Soc. A* **1950**, *204*, 406.

(30) Nelsen, S. F.; Blackstock, S. C.; Kim, Y., *J. Am. Chem. Soc.* **1987**, *109*, 677. Nelsen, S. F.; Yunta, M. J. R. *J. Phys. Org. Chem.* **1994**, *7*, 55.

(31) Leonhardt, H.; Weller, A. *Ber. Bunsen-Ges. Phys. Chem.* **1963**, *67*, 791.

(32) (a) Burshtein, A. I.; Ivanov, K. L. *Phys. Chem. Chem. Phys.* **2002**, *4*, 4115. (b) Gladkikh, V. S.; Burshtein, A. I.; Angulo, G.; Grampp, G. *Phys. Chem. Chem. Phys.* **2003**, *5*, 2581.

(33) Dabestani, R.; Ivanov, I. N. *Photochem. Photobiol.* **1999**, *70*, 10.

(34) Nickel, B.; Wilhelm, H. E.; Ruth, A. A. *Chem. Phys.* **1994**, *188*, 267.

(35) Lillie, E. D.;Van Ooteghem, D.; Levin, G.; Szwarc, M. *Chem. Phys. Lett.* **1976**, *41*, 216.